

# A General Route of Using Lignite Depolymerized Derivatives for Catalyst Construction: Insights into the Effects of the Derivative Structures and Solvents

Jianxiu Hao,\* Limin Han, Keli Yang, Na Li, Runxia He, Keduan Zhi, and Quansheng Liu\*

Cite This: *ACS Omega* 2021, 6, 14926–14937

Read Online

ACCESS |



Metrics &amp; More



Article Recommendations



Supporting Information

**ABSTRACT:** Depolymerization is an emerging and promising route for the value-added utilization of low-rank coal (LRC) resources, and how to use the complex depolymerized mixtures efficiently is of great importance for this route. In this work, we designed the rational route of using depolymerized mixtures from lignite *via* ruthenium ion-catalyzed oxidation (RICO) depolymerization directly without complex separation to construct a Zr-based hydrogenation catalyst. The prepared catalyst was applied into the catalytic transfer hydrogenation of biomass-derived carbonyl compounds. Meanwhile, a copper-based oxidation catalyst was also constructed via a similar route to investigate the universality of the proposed route. Special insights were given into how the depolymerized components with different structures influenced the performances of the catalysts. The effects of the solvents used during the catalyst preparation (H<sub>2</sub>O and DMF) were also studied. The results showed that the proposed route using the depolymerized mixtures from lignite *via* RICO to construct catalysts was feasible for both Zr-based and Cu-based catalysts. The two catalysts prepared gave high efficiency for their corresponding reaction, *i.e.*, the Zr-based catalyst for catalytic transfer hydrogenation of biomass-derived carbonyl compounds and the Cu-based catalyst for selective oxidation of alcohols into aldehydes. Different depolymerized components contributed differently to the activity of the catalyst, and the solvents during the preparation process could also influence the activity of the catalyst. The depolymerized components and the solvents influenced the activities of the Zr-based catalyst mainly *via* changing the Zr contents, the microenvironment of Zr<sup>4+</sup>, and the specific areas of the catalyst.



## 1. INTRODUCTION

As the reserves of fossil resources on earth are limited, the highly efficient and value-added utilization of fossil resources is of great importance.<sup>1,2</sup> Low-rank coals (LRCs) are important fossil resources with considerable accounts among the coal resources. LRCs have some disadvantages compared with high-rank coals (HRCs), such as the high contents of volatiles, instability in air, and low energy density, which limit severely the direct application of LRCs as energy sources.<sup>3–5</sup> However, the specific structures and properties make LRCs different from HRCs, providing humans new perspectives for utilizing LRCs based on their unique structures and properties. For example, the aromatic structures and oxygen-containing groups in LRCs make it possible to prepare fine chemicals and/or carbon-based materials from LRCs.<sup>6–8</sup> The route of degrading or depolymerizing low-rank coals into soluble fractions with much smaller molecular weights but maintaining the aromatic units has drawn extensive attention, and various processes have been developed to degrade LRCs. Valuable chemicals such as polyprotic acids (trimesic acid, pyromellitic acid, mellitic acid, succinic acid, etc.) could be obtained from the depolymerized mixtures.<sup>8–12</sup> Therefore, the utilization of LRCs via depolymerization is an emerging and promising route for the utilization of LRC resource. But up to now, most of the reported work

has focused on the development of new depolymerization processes or studying the structures of raw LRCs according to the structure information of the depolymerized products.<sup>13–17</sup> In contrast, much less focus has been paid on how to further utilize the depolymerized mixtures, which was obviously important for promoting the depolymerization route to practical application.

Due to the complexity of the depolymerized mixtures in the composition and contents of various products, two general routes are probable to utilize the depolymerized mixtures. (1) One route is extracting single or several valuable components with improved purity from the depolymerized mixtures via suitable separation or purification processes.<sup>18–21</sup> This route is highly attractive because various chemicals with added values were contained in the depolymerized mixtures, as stated above. Unfortunately, the depolymerized mixtures are so complex that the separation processes are not very easy or even

Received: February 10, 2021

Accepted: May 24, 2021

Published: June 4, 2021



cumbersome. Both the cost and the separation yield of the whole processes should be carefully evaluated, and extensive efforts are still highly desired on this aspect. (2) The other route to utilize the depolymerized mixtures is using the mixtures directly without tricky separation. Compared with the first route, this route is much simpler in processes and more feasible with no need for energy or solvent input during separation. Similar with the first route, studies on this aspect are still at the beginning stage, and more focus should be paid. Recently, we conducted some attempts on the direct use of LRCs or their derivatives without complex separation.<sup>22–26</sup> Humic acid (HA) mixtures extracted from LRC (typical lignite) by a diluted NaOH solution under mild conditions could be directly used to prepare Zr-based catalysts *via* the interaction of  $Zr^{4+}$  with the acidic groups in HA, and the catalyst showed high efficiency for the conversion of biomass-derived furfural or ethyl levulinate.<sup>22,25</sup> Further studies showed that the raw lignite could be used directly to construct a Zr-based catalyst by a similar route, and the pretreatment of demineralization *via* acid washing of lignite could improve the stability of the obtained catalyst.<sup>23</sup> These previous studies identified that the idea of the direct use of HA mixtures from lignite without separation and purification to construct a catalyst was feasible. However, only part of the soluble HA components could be extracted and used from the solid LRCs under mild conditions (low NaOH concentration and temperatures) in the above work, and the total utilizing efficiency of LRCs is still very low (around 30 wt % for lignite). The development of efficient depolymerizing methods of LRCs provides solutions for this problem because some of the methods such as ruthenium ion-catalyzed oxidation (RICO) could even convert LRCs totally into soluble fractions.<sup>13</sup> Because various carboxyl compounds were contained in the depolymerized mixtures *via* RICO, it was rational to speculate that the depolymerized mixtures could also be applied in the construction of catalysts through the interaction of metal ions with the functional groups. But to the best of our knowledge, it has not been reported whether the depolymerized mixtures from LRCs *via* RICO could be used directly to construct catalysts without complex separation or purification. How the depolymerized components of lignite influenced the activity of the obtained catalysts is still unknown. On the other hand, the depolymerization process was often conducted in water solution, and thus, water was the ideal solvent for catalyst preparation without the need for solvent replacement. But the commonly used solvents for the coordination of metal ions with carboxylate groups to construct metal–organic ligand hybrid catalysts were organic solvents (such as DMF). Therefore, the comparison analysis of different solvents for catalyst preparation is also required.

In this work, we designed rationally the route of using the depolymerized mixtures from lignite *via* RICO depolymerization to construct a Zr-based hydrogenation catalyst for hydrogenation reactions. The route was proposed based on the condition of (1) high efficiency of RICO for depolymerizing lignite and (2) the abundance of acidic functional carboxyl groups in the depolymerized products. A Cu-based catalyst was also constructed and applied into oxidation reactions to check the universality of this route. Special focus was given to how the depolymerized components with different structures contributed to the performances of the catalysts and the effects of the solvents ( $H_2O$  and DMF) during the preparation of the catalysts. The results showed that it was feasible to use

the depolymerized mixtures from lignite *via* RICO to construct catalysts. Two kinds of catalysts gave high efficiency for their corresponding reaction, including a Zr-based catalyst for catalytic transfer hydrogenation of carbonyl compounds and a Cu-based catalyst for selective oxidation of alcohols. These results showed that the route was robust with broad applicability. The different depolymerized components and solvents had significant influences on the activity of the Zr-based catalyst, mainly *via* changing the Zr contents, the microenvironment of  $Zr^{4+}$ , and the specific areas of the catalyst. The proposed route in this paper may be a chance for the utilization of LRC and catalyst preparation with the advantages of high efficiency of the catalysts, broad applicability, and simple preparing processes.

## 2. RESULTS AND DISCUSSION

### 2.1. Preparation and Application of the Zr-DM Catalyst.

**2.1.1. Studies of the Preparation Conditions and Reaction Conditions of the Zr-DM Catalyst.** It is too difficult to accurately calculate the content of the acidic functional groups of DM due to the complexity of composition, so the dosage of DM was difficult to determine during the catalyst preparation. In this work, the appropriate dosage of DM was studied *via* changing the mass ratio of the zirconium precursor to DM. Different catalysts were prepared with the mass ratio of  $ZrOCl_2 \cdot 8H_2O$ /DM corresponding to 0:1, 0.1:1, 0.5:1, 1:1, 2:1, and 4:1, respectively. The optimal mass ratio of zirconium precursors to the depolymerized products was chosen according to the state of the supernatant after the solid precipitates were formed and centrifuged. The color of supernatant was different when the amount of  $ZrOCl_2 \cdot 8H_2O$  changed (Figure 1). The DM was dissolved well in the

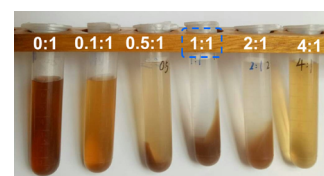


**Figure 1.** Optical images of Zr-DM catalysts prepared at different mass ratios of  $ZrOCl_2 \cdot 8H_2O$  to DM. Preparation condition: 80 °C, 5 h; centrifugation conditions: 1250 rpm, 1 min.

deionized water without zirconium precursor addition and formed a brown homogeneous solution (0:1). When DM was directly used as the catalyst, the substrate furfural could not be transformed, indicating that DM itself had no catalytic activity. With the increase of the amount of  $ZrOCl_2 \cdot 8H_2O$ , the gel-like precipitate was formed. After centrifugation, the color of the super liquid changed from brown to colorless and transparent (1:1), indicating that the zirconium precursor was completely coordinated with the carboxylic acid in DM to form precipitation. With the increase of the dosage of the zirconium precursor, the supernatant became brown again (2:1 and 4:1), indicating that some of the depolymerized products were not coordinated with  $Zr^{4+}$ . This may be due to the stronger acidity of the solution under the higher dosage of zirconium precursor. Considering the utilization efficiency of organic components in DM and the zirconium precursor, the ratio of 1:1 was selected during the catalyst preparation for further study.

The influences of reaction parameters on the catalysts were investigated, including the catalyst dosage, reaction temper-

ature, and reaction time. As shown in Figure 2a, the conversion of furfural and the yield of furfuryl alcohol increased with the

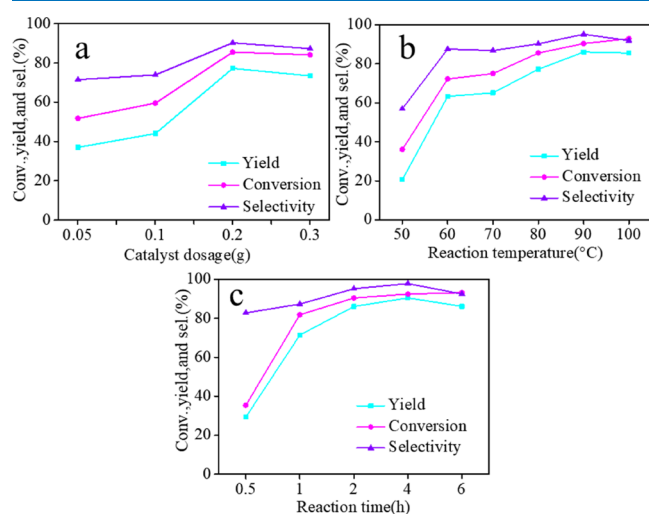


**Figure 2.** The influences of reaction parameters on the performance of catalysts. (a) Effect of the Zr-DM catalyst dosage. (b) Effect of the reaction temperature. (c) Effect of the reaction time.

increase of the catalyst dosage from 0.05 to 0.2 g. Using the catalyst dosage of 0.2 g, the conversion, yield, and selectivity were 85.6, 72.3, and 90.3%, respectively. However, if the dosage of the catalyst increased to 0.3 g, both the conversion and the product yield had a slightly downward trend. The reaction system presented a phase of slurry when the amount of catalyst was in excess of 0.2 g, resulting in the poor dispersion of the catalyst particles that might have a negative effect on mass transportation during the reaction. The appropriate catalyst dosage was 0.2 g in the present reaction conditions and was used in the subsequent experimental study. The temperature had a significant influence on the performance of the Zr-DM catalyst as shown in Figure 2b. Before 90 °C, the conversion of furfural and the yield of furfuryl alcohol increased significantly with the increase of temperature, reaching 90.4 and 86.1%, respectively, under 90 °C. However, as the temperature continued to rise, although the conversion continued to increase at a slower rate, the yield and selectivity declined slightly, presumably due to the formation of some byproducts, which could be proved by the deep color of the reaction system under 100 °C. Therefore, 90 °C was determined to be the suitable temperature for subsequent investigations. Under the above reaction conditions, the time profile of the reaction was studied, as shown in Figure 2c. The conversion of furfural and the yield of furfuryl alcohol increased significantly when the reaction time extended. The conversion and selectivity increased slightly and reached the maximum value (conversion 92.5%, selectivity 97.8%) when the reaction time was extended to 4 h. As the reaction time was extended to 6 h, the yield and selectivity began to decline, which may be due to the fact that the extension of the reaction time led to the formation of the condensation byproducts of alcohol and aldehyde. This could be proven by the presence of some weak and unknown peaks during GC detection.

Reaction conditions: furfural (1 mmol), isopropanol (5 mL). (a) 80 °C, 2 h. (b) Catalyst 0.2 g, 2 h. (c) Catalyst 0.2 g, 90 °C.

**2.1.2. Comparison of the Zr-DM Catalyst with Other Catalysts.** The activity of the prepared Zr-DM catalyst was compared with that of typical Zr-based transfer hydrogenation catalysts in the literature, as shown in Table 1. By comparing

**Table 1. Comparison of Zr-DM Catalyst with Typical Metal Catalysts in the Literature for the Conversion of Furfural<sup>a</sup>**

entry	catalysts	reaction conditions	C (%)	Y (%)	S (%)	refs
1	Zr-DM	IPA, 90 °C, 2 h	90.4	86.1	95.2	this work
2	Zr-RSL	IPA, 90 °C, 6 h	93.4	80.9	86.7	23
3	Zr-SBA-15	IPA, 90 °C, 6 h	50.0	40.0	80.0	27
4	Zr-TMSA	IPA, 70 °C, 5 h	93.6	89.5	95.6	28
5	Zr-HAs	IPA, 50 °C, 15 h	97.4	96.9	99.0	29
6 <sup>b</sup>	Zr-PhyA	IPA, 100 °C, 2 h	99.3	99.3	100.0	30
7 <sup>c</sup>	ZrPN	IPA, 100 °C, 15 h	93.0	90.0	96.8	31
8 <sup>d</sup>	$\gamma$ -Fe <sub>2</sub> O <sub>3</sub> @HAP	IPA, 180 °C, 3 h	96.2	91.7	95.3	32
9 <sup>e</sup>	Fe/NC	IPA, 160 °C, 15 h	91.6	76.0	83.0	33
10 <sup>f</sup>	Ni-Cu/Al <sub>2</sub> O <sub>3</sub>	IPA, 200 °C, 4 h	95.4	95.4	100	34
11	MgO	IPA, 170 °C, 5 h	100.0	74.0	74.0	35

<sup>a</sup>C: conversion of furfural, Y: yield of FAL, S: selectivity of FAL, IPA: isopropanol alcohol. <sup>b</sup>Zr-PhyA: Zr-phytic acid hybrid. <sup>c</sup>Zr-PN: organotriphosphate-zirconium hybrid. <sup>d</sup>Hydroxyapatite-encapsulated magnetic  $\gamma$ -Fe<sub>2</sub>O<sub>3</sub>. This reaction was a metal-free catalysis process, and the amounts of the active sites were not mentioned in the literature. <sup>e</sup>Fe/NC: nitrogen-doped carbon-supported iron. <sup>f</sup>Ni-Cu/Al<sub>2</sub>O<sub>3</sub>: The amounts of the active sites were Ni.

entries 1–7 of Table 1, it can be seen that the reaction conditions of all Zr-based catalysts were relatively mild. Under the similar reaction condition, the conversion and product selectivity of the prepared Zr-DM catalyst were similar to those of typical Zr-catalysts. In addition, other transition metal-based transfer hydrogenation catalysts (e.g., Fe, Ni, and Mg) were listed in entries 8–11 of Table 1. These catalysts usually require higher temperatures to achieve conversions and yields close to those of zirconium-based catalysts.

For the selective conversion of furfural to furfuryl alcohol, there are usually two paths: one is the catalytic transfer hydrogenation reaction with isopropanol or formic acid as the hydrogen source, and the other is the direct hydrogenation reaction with hydrogen as the hydrogen source.<sup>36</sup> Precious metal catalysts<sup>37,38</sup> and transition metal catalysts<sup>39–41</sup> were usually used in the hydrogenation path with H<sub>2</sub> as the hydrogen source, in which the noble metal catalyst usually showed higher efficiency and TOF value than the transition metal catalyst under mild reaction conditions. However, whether using noble metal catalysts or transition metal catalysts, this path needed to be carried out at high pressures.<sup>37,42,43</sup> Therefore, compared with the transition metal catalyst using H<sub>2</sub> as the hydrogen source, the Zr-DM catalyst prepared in this work had a similar reaction effect to it, but the reaction conditions were milder. From the comprehensive comparison of reaction conditions, raw material cost, convenience in the preparation process, catalyst cost, and so on, the Zr-DM catalyst constructed in this work

had certain advantages compared with precious metals and other transition metal catalysts.

**2.1.3. Structure Characterization of the Zr-DM Catalyst.** Detailed characterizations were conducted by SEM-EDS, XRD, FTIR, XPS, and TG (Figure 3) to understand the structures of

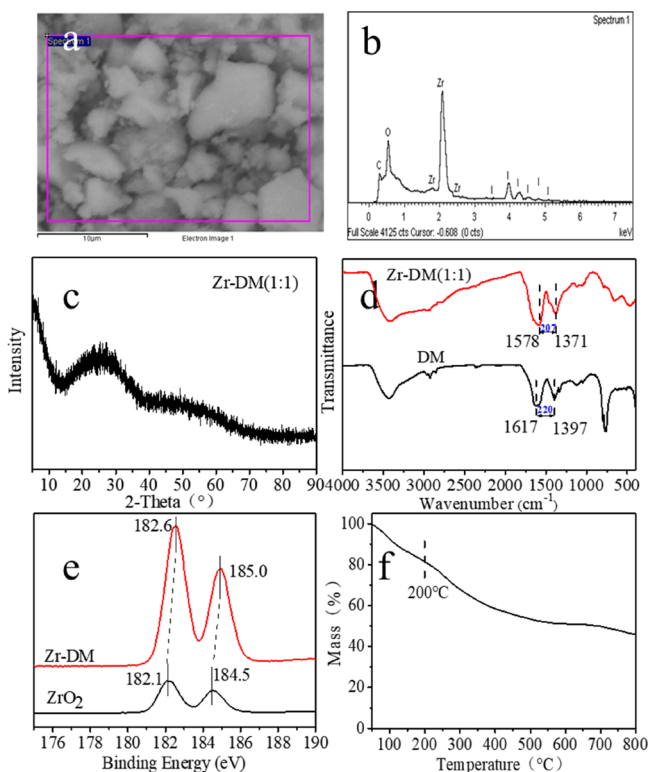
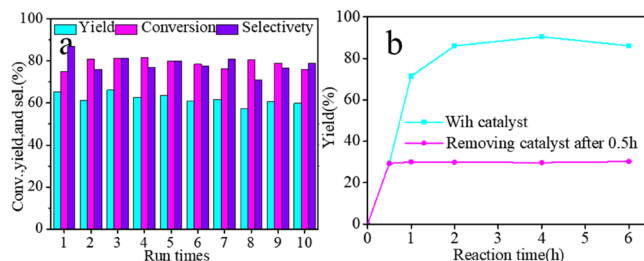


**Figure 3.** Characterization of the as-prepared Zr-DM catalyst by SEM (a), EDS (b), XRD pattern (c), FTIR spectra (d), XPS spectrum (e), and TG analysis (f).

Zr-DM. SEM showed that the Zr-DM catalyst was composed of particles with no uniform shapes (Figure 3a). EDS mapping showed a strong Zr signal for the catalyst after the interaction of  $Zr^{4+}$  with DM (Figure 3b), showing that the Zr element was successfully introduced into the catalyst. The XRD pattern of Zr-DM showed a broad peak around  $2\theta = 25^\circ$ , indicating that the catalyst had an amorphous structure (Figure 3c). The FTIR spectra of DM and the Zr-DM catalyst were compared in Figure 3d. It can be seen that the wavenumber between the characteristic asymmetric vibrations (DM,  $1617\text{ cm}^{-1}$ ; Zr-DM,  $1578\text{ cm}^{-1}$ ) and the symmetric vibrations (DM,  $1397\text{ cm}^{-1}$ ; Zr-DM,  $1371\text{ cm}^{-1}$ ) of the carboxylate groups was narrowed from  $220\text{ cm}^{-1}$  for DM to  $207\text{ cm}^{-1}$  for Zr-DM, proving that  $Zr^{4+}$  ions were coordinated to carboxylate groups in DM.<sup>44</sup> The chemical environment of Zr species in Zr-DM was detected by the Zr 3d XPS. Compared with  $ZrO_2$ , the binding energy peaks of Zr 3d<sub>5/2</sub> and Zr 3d<sub>3/2</sub> moved from 182.1 and 184.5 eV ( $ZrO_2$ ) to 182.6 and 185.0 eV (Zr-DM), respectively (Figure 3e). The higher binding energy of Zr 3d indicated a higher positive charge on the Zr atoms, resulting in a stronger Lewis acidity of Zr. The higher acidity of Zr species could improve the activity of the Zr-DM catalyst.<sup>45</sup> TG analysis showed that the prepared catalyst had a low weight loss of 14% at  $200^\circ\text{C}$  resulting from the desorption of water and ethanol adsorbed on the catalyst. The weight loss after  $300^\circ\text{C}$  may be due to the decomposition of side chains and small molecules in

Zr-DM, and the total weight loss of the catalyst was around 50% at  $800^\circ\text{C}$ . The catalyst exhibited good stability at the reaction temperature below  $200^\circ\text{C}$  (Figure 3f). The characterization results showed that the Zr element was successfully coordinated with the carboxylate groups in DM, and Zr existed in the form of coordination structures with carboxylate groups.

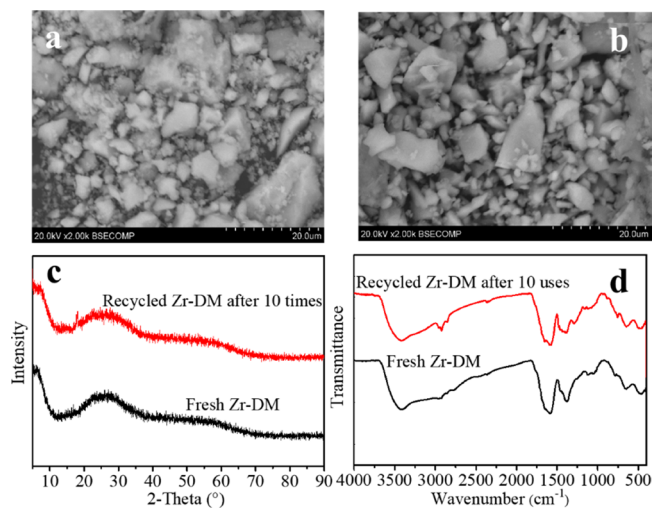
**2.1.4. Reusability and Substrate Scope Expansion of Zr-DM Catalysts.** Reusability and heterogeneity were important for the solid heterogeneous catalyst. The reusability results showed that there was no considerable decrease in the conversion, yield, and selectivity after 10 cycles for Zr-DM compared to the first use (Figure 4a), indicating that the



**Figure 4.** Reusability(a) and heterogeneity(b) of the prepared catalyst. Reaction conditions: furfural 1 mmol, isopropanol 5 mL, Zr-DM 0.2 g, reaction temperature  $70^\circ\text{C}$  ( $90^\circ\text{C}$  for b), and reaction time 2 h.

catalyst could be reused and was very stable. The heterogeneity of the catalyst was also studied, and the results confirmed that the active sites in Zr-DM did not leach into the reaction mixture, and it was a heterogeneous catalyst (Figure 4b).

The structures of the Zr-DM catalyst recovered after 10 cycles were characterized and compared with the freshly prepared catalysts (Figure 5). As can be seen from the SEM characterization, the morphology of the recycled catalyst (Figure 5b) was irregular and granular, which was similar to that of the fresh catalyst (Figure 5a). XRD results showed that the catalyst had no obvious diffraction peaks and was still amorphous after use (Figure 5c). FTIR showed that the

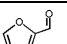
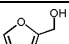
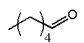
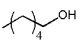
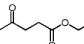
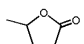
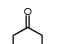
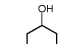
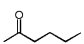
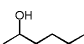
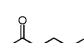
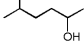



**Figure 5.** Comparison of the freshly prepared and recycled Zr-DM catalysts after 10 reuses. SEM of the fresh (a) and recycled catalyst (b), FTIR spectra (c), and XRD patterns (d).

recycled catalyst had a similar spectrum to the fresh catalyst (Figure Sd). These results proved that the catalyst had excellent structure stability.

Encouraged by the excellent performance of the Zr-DM catalyst on the catalytic hydrogenation of furfural, we applied the catalyst into other carbonyl compounds with different structures to investigate the universality of Zr-DM catalyst for different substrates. The results were shown in Table 2. It can

**Table 2. Conversion of Different Carbonyl Compounds over the Zr-DM (1:1) Catalyst**

Entry	Reactant	Product	T (°C)	t (h)	Conv. (%)	Yield (%)	Sel. (%)
1			90	4	92.5	90.0	97.3
2			100	16	95.7	81.7	85.4
3			160	12	95.3	90.8	95.3
4			120	5	95.7	85.1	88.9
5			160	16	94.2	80.6	85.6
6			140	10	89.7	76.6	85.4
						6.4	7.1

<sup>a</sup>Reaction conditions: substrate 1 mmol, isopropanol 5 mL, Zr-DM (1:1) 0.2 g, and other conditions as stated in the table.

be seen that Zr-DM had good activity for the studied compounds. The reaction temperature and reaction time for different substrates were different, but the conversion of each substrate could reach more than 90% under the optimized conditions, indicating that the Zr-DM catalyst had a wide range of substrate applicability.

## 2.2. Catalyst Expansion: Cu-DM Oxidation Catalyst.

The above studies showed that the proposed route of constructing a catalyst using DM was feasible for the Zr-based hydrogenation catalyst. It is desirable to see if this route was also feasible for other types of catalysts. Encouraged by this idea, we applied the route to construct a Cu-based catalyst, an oxidative catalyst commonly used for selective oxidation of alcohols into carboxylic acids. The preparation process of Cu-DM was similar to that of Zr-DM, and the preparation conditions were also optimized (Figure S1 and Table S1). Under the mass ratio of Cu precursor ( $\text{Cu}(\text{CH}_3\text{COO})_2 \cdot \text{H}_2\text{O}$ ) to DM of 2:1, the obtained Cu-DM catalyst gave a higher activity (Table S1).

The structures of Cu-DM were characterized by SEM-EDS, XRD, FTIR, XPS, and  $\text{N}_2$  adsorption–desorption, and the discussion concerning the structures was in the Supporting Information (Figure S2). Herein, the performances of the Cu-DM catalyst were discussed in detail. The influences of the reaction conditions were shown in Figure 6.

The effect of the Cu-DM catalyst dosage on the oxidation reaction of benzyl alcohol was shown in Figure 6a. When the catalyst dosage was 0.04 g, the conversion and yield of the reaction reached over 40%, indicating that the Cu-DM (2:1) catalyst had high activity, and moderate conversion and yield

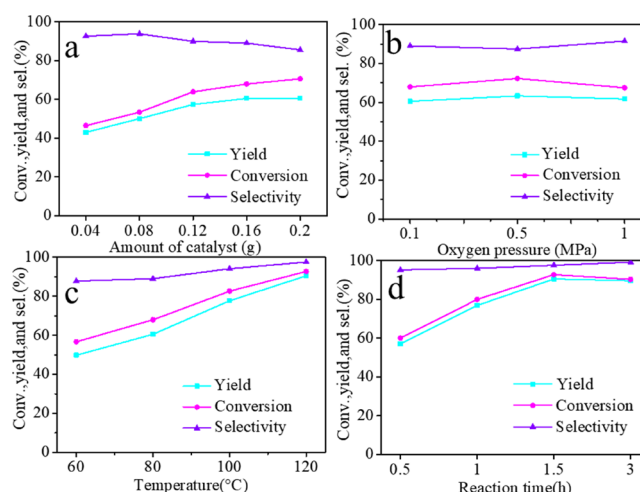


**Figure 6.** The influences of reaction parameters on the performance of the Cu-DM catalyst: (a) catalyst dosage, (b)  $\text{O}_2$  pressure, (c) reaction temperature, and (d) reaction time.

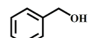
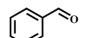
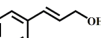
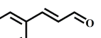
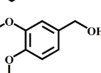
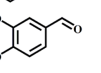
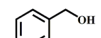
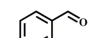
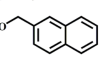
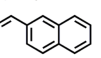
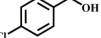
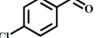
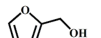
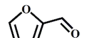
could be achieved by adding a small amount of the catalyst. When the catalyst dosage reached 0.16 g, the conversion of benzyl alcohol reached 67.9%, the yield of benzaldehyde reached 60.5%, and the selectivity reached 89.0%. The catalyst dosage continued to be increased to 0.2 g, and the conversion of benzyl alcohol increased to 70.6%. However, the yield of benzaldehyde did not increase and the selectivity decreased, which may be caused by the uneven mass transfer of the excessive catalyst in the limited reaction volume. In the following work, 0.16 g was selected as the appropriate dosage of catalyst. Oxygen plays an important role in the selective oxidation of benzyl alcohol. Under the condition of a catalyst dosage of 0.16 g and reaction temperature and time of 80 °C and 1.5 h, respectively, oxygen at different initial pressures was filled into the reaction system to investigate the influence of oxygen pressure on the reaction. The experimental results were shown in Figure 6b. It can be seen from the figure that when the oxygen pressure in the reactor was increased from 0.1 to 1.0 MPa, the conversion of benzyl alcohol and the yield of benzyl formaldehyde did not change much and were basically at the same level. It showed that the oxygen atmosphere of 0.1 MPa could make the reaction conversion and yield reach a high level, which was enough to meet the demand of oxygen for the catalytic oxidation reaction under the studied reaction conditions. The reaction temperature of Cu-DM (2:1) catalyzed oxidation of benzyl alcohol was investigated, as shown in Figure 6c. As can be seen from the figure, when the reaction temperature increased from 60 to 120 °C, the conversion of benzyl alcohol and the yield of benzaldehyde showed a linear upward trend. At 120 °C, the conversion of benzyl alcohol reached 92.7%, and the yield of benzaldehyde came to 90.5%. With the increase in temperature, the product selectivity increased slowly. Considering energy saving and keeping a high yield of the target product, 120 °C was selected as the optimal reaction temperature for the catalytic oxidation reaction of the catalyst in the following research. The reaction time of catalytic oxidation was investigated, as shown in Figure 6d. The results showed that under the above conditions, the conversion of benzyl alcohol and the yield of benzyl formaldehyde could reach more than 57% after 0.5 h of reaction, and they could reach more than 80% when the reaction time was extended to 1 h. After 1.5 h extension, the

conversion of benzyl alcohol, the yield of benzaldehyde, and the selectivity reached the maximum values, which were 92.7, 90.5, and 97.6%, respectively. The conversion and yield changed little when the reaction time was further prolonged. Therefore, the appropriate time for the reaction was determined to be 1.5 h under the present reaction conditions.

Reaction conditions: benzyl alcohol (1 mmol), TEMPO (0.5 mmol), Na<sub>2</sub>CO<sub>3</sub> (1 mmol), DMF (5 mL). (a) 80 °C, 0.1 MPa, and 90 min. (b) 80 °C, 90 min, and catalyst 0.16 g. (c) 0.1 MPa, 90 min, and catalyst 0.16 g. (d) 0.1 MPa, catalyst 0.16 g, and 120 °C.

To investigate the applicability of the Cu-DM catalyst for different alcohols, the performances of the Cu-DM catalyst for selective oxidation of different alcohols studied and the results were summarized in Table 3. The results showed that the

**Table 3. Aerobic Oxidation Reaction of Various Alcohol Compounds over the Cu-DM Catalyst<sup>a</sup>**

Entry	Reactant	Product	T (°C)	t (h)	Conv. (%)	Yield (%)	Sel. (%)
1			120	1.5	92.7	90.5	97.6
2			100	9	98.9	94.5	95.6
3			110	5	98.3	96.7	98.4
4			100	8	96.9	89.1	91.9
5			100	7	93.6	91.9	98.2
6			100	6	96.8	95.9	99.1
7			100	10	89.4	84.6	94.6

<sup>a</sup>Reaction conditions: alcohol (1 mmol), catalyst (160 mg), TEMPO (0.5 mmol), Na<sub>2</sub>CO<sub>3</sub> (1 mmol), DMF (5 mL), and O<sub>2</sub> (0.1 MPa).

reaction temperature and time required for different alcohols were different, but the conversion and yield could reach about 90% under the preliminarily optimized reaction conditions, which indicated that the Cu-DM catalysts had good applicability for the selective oxidation of alcohols with different structures.

The reusability and heterogeneity of Cu-DM catalyst were investigated (Figure S3). The results showed that the Cu-DM catalyst could be reused for at least five cycles without a considerable decrease in the conversion and yield. After the removal of the solid catalyst during the reaction, the yield did not further increase, indicating that it was the solid catalyst to catalyze the reaction and the catalytic process was heterogeneous. The recycled catalyst was characterized by SEM, XRD, and FTIR and compared with the fresh Cu-DM catalyst (Figure S4). The results showed that the structures of Cu-DM catalyst had no obvious changes after five uses, indicating that the catalyst had excellent structure stability. The comparison of the Cu-DM catalyst with other catalysts was shown in Section S3. It can be seen that the catalyst has a potential to be competitive with the analogues reported in the literature.

**2.3. Effects of the Depolymerized Components on the Performance of the Catalysts.** **2.3.1. Performance of Catalysts Prepared by Different Components.** Due to the complexity of the DM from lignite, we further studied the

contributions and influences of different components in DM on the activities of the catalysts. The depolymerized products mainly include small molecular fatty acids and various kinds of phenyl carboxylic acids. These carboxylic acids have different structures and physical or chemical properties, and their concentrations in the depolymerized products are also different. Thirteen typical organic acids in the depolymerized products of lignite *via* RICO were used to prepare Zr- and Cu-based catalysts, respectively, to investigate the contributions and influences of different components in DM on the activity of the catalysts constructed.

Reaction conditions: furfural (1 mmol), isopropanol (5 mL), 70 °C, 5 h, and catalyst 0.2 g.

For the Zr-based catalyst, it can be seen from Figure 7 that the activity of Zr-based catalysts prepared by different phenyl

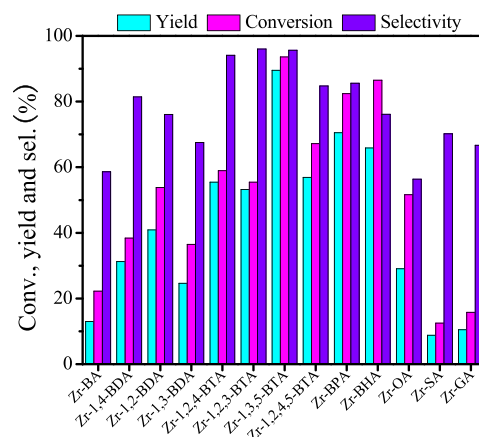


**Figure 7.** The activity of zirconium-organic acid catalysts prepared using different carboxylic acids.

carboxylic acids and fatty acids was different, and the activity of the catalysts prepared by phenyl carboxylic acids was generally higher than that of catalysts prepared by fatty acids. With the increasing number of carboxyl groups in phenyl carboxylic acids, the activity of the catalysts had an increasing trend. For the benzoic acid isomers with the same number of carboxyl groups, the activity of the catalysts prepared using different isomers was also different. Taking benzene tricarboxylic acid (BTA) as an example, the catalyst prepared using 1,3,5-BTA as the organic ligands gave higher activity than the catalysts prepared using 1,2,3-BTA and 1,2,4-BTA. For the studied fatty acids, the activity of the catalysts had a relationship with the length of the carbon chain in the acids. Zr-OA (C2) had higher activities than Zr-SA (C4) and Zr-GA (C5).

For the Cu-based catalyst, the activity of the catalysts prepared using different phenyl carboxylic acids and fatty acids was also different (Figure 8), but the changing trends of the activity were different from Zr-based catalysts. The activity of the Cu-based catalysts showed first an increasing and then a decreasing trend with the increasing number of carboxyl groups in phenyl carboxylic acids, with Cu-1,2-BDA giving the best performance. The catalysts prepared using fatty acids (Cu-OA and Cu-SA) also had good activity, and the activity of Cu-SA (C4) was higher than that of Cu-OA (C2).

The above results proved that the various organic acids in DM from lignite could contribute to the activity of Zr-based or Cu-based catalysts, but different components contributed to different extents. The contributions of different components

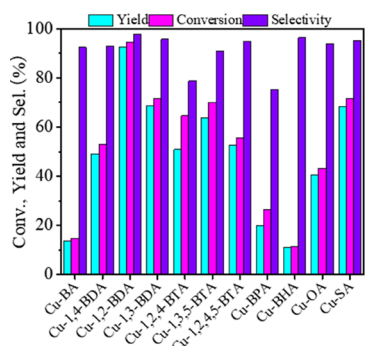


**Figure 8.** The activity of copper-based catalysts prepared using different organic acids.

also had a relationship with the types of the catalysts. This phenomenon could be caused by various factors such as the interactions of the organic acids with the metal ions and the contents of metal ions in the prepared catalysts.

Reaction conditions: benzyl alcohol 1 mmol, catalyst 160 mg, TEMPO 0.5 mmol,  $\text{Na}_2\text{CO}_3$  1 mmol, and DMF 5 mL.  $\text{O}_2$ : 0.1 MPa. 60 °C and 4 h.

**2.3.2. Discussion about the Reason for the Different Catalytic Activity of the Catalysts from Different Components.** Zr-based catalysts were taken as examples to discuss the reason for the different catalytic activity of the catalysts prepared using different components. Several representative Zr-based catalysts prepared using different organic acids were characterized by BET, ICP, and XPS, respectively. The results were shown in Table 4 and Figure 9. It can be found that the

**Table 4. Comparison of the Specific Area and Zr Contents among Zr-Based Catalysts Prepared with a Variety of Organic Acids**

entry	catalysts	Zr cont. wt %	BET surface area ( $\text{m}^2/\text{g}$ )
1	Zr-DM	29.8	219.7
2	Zr-1,3-BDA	27.9	17.8
3	Zr-1,3,5-BTA	48.1	25.2
4	Zr-1,2,4,5-BA	21.6	28.5
5	Zr-BPA	34.5	180.1
6	Zr-BHA	49.6	234.9

zirconium mass content of Zr-1,3,5-BTA, Zr-BPA, and Zr-BHA (48.1, 34.5, and 49.6%, respectively) was higher than that of Zr-1,3-BDA and Zr-1,2,4,5-BA (27.9 and 21.6%, respectively). So, the high zirconium content may be one reason for the high

activity of these catalysts (Zr-1,3,5-BTA, Zr-BPA, and Zr-BHA). In addition, BET results showed that the specific surface area of Zr-BPA and Zr-BHA catalysts was much higher than that of other catalysts. The presence of a high specific surface area was conducive to the contact between the substrate and the active site of the catalyst, thus improving the catalytic activity.

Figure 9a showed the Zr 3d spectrum of zirconium catalyst with aromatic carboxylic acid as the ligand. It can be seen from the figure that the Zr 3d binding energy of Zr-1,3,5-BTA was similar to that of Zr-DM, i.e., 182.6 and 185 eV, higher than that of other catalysts. The higher the binding energy of Zr 3d was, the higher the electropositivity of zirconium atoms, resulting in the stronger Lewis acid property of zirconium in the catalyst, which was conducive to the activation of carbonyl groups, thus improving the reaction rate. This may be one of the reasons why the activity of the Zr-1,3,5-BTA catalyst was higher than that of other catalysts. Figure 9b showed the O 1s XPS diagram of each catalyst with benzyl carboxylic acid as the ligand. It can be seen from the figure that, except for the O 1s binding energy of the Zr-1,3-BDA catalyst, the O 1s binding energy of Zr-based catalysts prepared by all benzene carboxylic acids was the same, 531.4 eV, which was lower than that of the Zr-1,3-BDA catalyst. The low binding of O 1s in the catalyst can make the O atom have higher electronegativity, thus improving the alkalinity of O and facilitating the decomposition of the hydroxyl group of isopropanol more easily, resulting in improved catalytic efficiency. This may be the reason why the catalytic activity of Zr-1,3-BDA was lower than that of other zirconium carboxylate catalysts. In general, high zirconium content, large specific surface area, and high acidity of zirconium and alkalinity of oxygen are more conducive to the improvement of catalyst activity and contribute more to the activity of Zr-DM.

**2.4. Effects of the Solvents on the Performances of the Zr-DM Catalysts.** Water is often used as the common solvent for the oxidative depolymerization of lignite, and the obtained depolymerized products exist in water. Therefore, the ideal solvent for constructing catalysts using the depolymerized products is water because this can avoid the solvent replacement from water to organic solvents. From the viewpoint of the preparation of the catalysts, organic solvents such as DMF were also commonly adopted. Therefore, in the further studies, we prepared Zr-DM catalysts both in water and in organic solvent (DMF) and compared their activities (Table 5). It can be seen that the Zr-DM catalyst prepared in water had higher activity, with higher conversion, yield, and TON

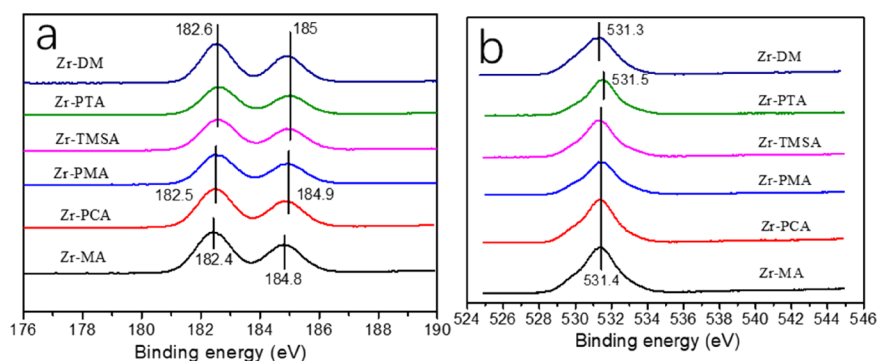


**Figure 9.** XPS spectra of (a) Zr 3d and (b) O 1s peak of the Zr-DM catalysts prepared using different organic acids.

**Table 5. Comparison of the Performances of the Different Zr-DM Catalysts Prepared in Water and in DMF<sup>a</sup>**

entry	catalysts	Zr cont. wt % (mol%)	BET surface area (m <sup>2</sup> /g) <sup>b</sup>	conv. (%)	yield (%)	sel. (%)	TON <sup>c</sup>
1	Zr-DM (H <sub>2</sub> O)	29.8	219.7	91.6	86.7	94.7	1.32
2	Zr-DM (DMF)	23.1	6.1	55.1	46.3	83.9	0.98

<sup>a</sup>Reaction conditions: furfural 1 mmol, isopropanol 5 mL, catalyst dosage 200 mg, reaction temperature 70 °C, and reaction time 5 h.

<sup>b</sup>Surface area based on the multipoint BET method. <sup>c</sup>The values of TON (turnover number) are the mole ratio of the product to the Zr element in the catalysts.

number than those of the Zr-DM catalyst prepared in DMF. This result further proved that the solvent could indeed influence the activity of the catalyst. Water was seen as an ideal solvent for preparing the Zr-DM catalyst not only due to no need for solvent replacement but also due to the higher activity of the Zr-DM catalyst prepared in water.

The reasons for the influences of the solvent on the activity were analyzed by characterizing the Zr-DM catalysts prepared in water and DMF, including ICP, N<sub>2</sub> adsorption–desorption, and XPS (Table 5 and Figures 10 and 11). ICP analysis showed that the zirconium content of the catalyst prepared in DMF was slightly lower than that of the catalyst prepared in water. BET results showed that the specific surface area of the catalyst prepared in water was much higher than that prepared in DMF (Table 5). The nitrogen adsorption–desorption isotherms of these two catalysts showed that the catalyst prepared in water was a type IV isotherm, with hysteresis loops characteristic of mesoporous materials centered around 11.2 nm, but the catalyst prepared in DMF was nonporous (Figure 10). The presence of mesoporous and high specific surface area was conducive to the contact of the substrate with the active sites in the catalyst, thus improving the reaction activity of catalysts. As seen from Zr 3d XPS, compared with the Zr-DM prepared in DMF, the Zr 3d binding energy of Zr-DM prepared in water had a higher binding energy level (Figure 11). The higher binding energy of Zr 3d indicated a higher positive charge on the Zr atoms, resulting in a stronger Lewis acidity of Zr. The higher acidity of Zr species could improve the activity of the Zr-DM catalyst.<sup>29</sup> This result together with the specific physical structures contributed to the higher activity of the Zr-DM catalyst prepared in water. Based on these results, it could be speculated that the solvents during the preparation process of the catalyst could affect the coordina-

tion role of Zr<sup>4+</sup> with the carboxylate groups in DM, leading to the different microstructures of the two catalysts and thus different catalytic performance.

### 3. CONCLUSIONS

In summary, a route of using the depolymerized mixtures (DMs) from lignite *via* RICO depolymerization without cumbersome separation to construct Zr-DM and Cu-DM catalysts was identified. Special attention was paid to the contribution of different components in DMs to the activity of the catalysts and the influences of the solvent during catalyst preparation on the performance of the catalyst. Both of the prepared Zr-DM and Cu-DM catalysts were proved to be highly active for their corresponding reaction, the catalytic transfer hydrogenation of carbonyl compounds and selective oxidation of alcohols, indicating that the route had broad applicability for different types of catalysts. The contribution of different depolymerized components on the activity of the catalyst depended on both the structures of the depolymerized components and the types of the catalysts. The solvent used for catalyst preparation could influence the activity of the obtained catalyst. For the Zr-DM catalyst, water was superior to DMF and could be used as the solvent directly without solvent replacement. Zr-DM prepared in water gave higher activity than Zr-DM prepared in DMF. The solvents influenced the activities of the Zr-based catalyst mainly *via* changing the Zr contents, the microenvironment of Zr<sup>4+</sup>, and the specific areas of the catalyst. The proposed route in this work may find its potential applications in the field of LRC utilization with the advantages of high efficiency of the catalysts, broad applicability, and simple preparing processes.

### 4. EXPERIMENTAL SECTION

**4.1. Materials.** Furfural (99%), furfuryl alcohol (98%), benzyl alcohol (99.5%), benzaldehyde (98%), ZrOCl<sub>2</sub>·8H<sub>2</sub>O (AR), 2,2,6,6-tetramethylpiperidine-1-oxyl (TEMPO, 98%), small-molecule fatty acids, multiple benzene polycarboxylic acids, and different aldehyde compounds were provided by J&K Scientific Ltd. Copper(II) acetate monohydrate(98%) was obtained from Acros. Different alcohol compounds were obtained from Alfa Aesar and Ark Pharm. Isopropanol (AR), ethanol (AR), KOH (AR), decane (AR), and other chemicals were provided by the Beijing Institute of Chemical Reagent. The raw lignite sample was obtained from Shengli Coalfield in Inner Mongolia, China. The as-received lignite sample was processed to meet experimental requirements.

**4.2. Catalyst Preparation.** **4.2.1. Depolymerization of Lignite.** The method of RICO was chosen to depolymerize

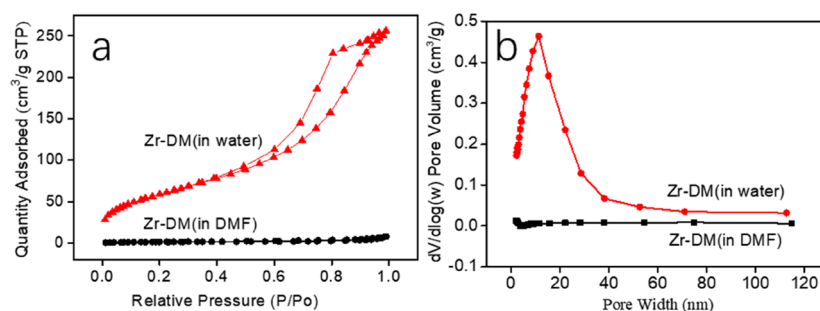


**Figure 10.** Comparison chart of N<sub>2</sub> adsorption–desorption isotherm (a) and pore size distribution (b) of the synthesized Zr-DM catalysts in water and DMF, respectively.



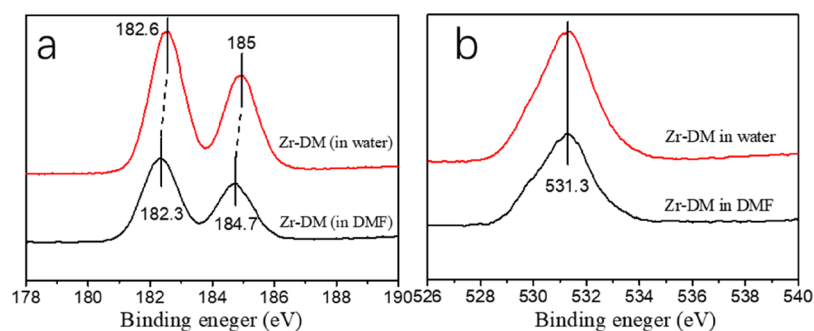


**Figure 11.** XPS spectra of (a) Zr 3d and (b) O 1s peak of the Zr-DM catalysts synthesized in water and DMF, respectively.

lignite due to its mild reaction conditions and high depolymerization efficiency. To avoid the possible influences of inherent minerals on the catalysts, the demineralized lignite was used to obtain the depolymerized mixtures. The demineralization process was described in detail in our previous reports.<sup>26,46</sup> The RICO process was the same as the reported literature.<sup>7</sup> The typical process was as follows: 50 mg of  $\text{RuCl}_3$ , 2 g of demineralized lignite, 50 mL of  $\text{CH}_3\text{CN}$ , 50 mL of  $\text{CCl}_4$ , and 75 mL of the distilled water were put into a 250 mL spherical flask and magnetically stirred at 35 °C for 2 h to afford reaction mixture 1 (RM1). Then, 16 g of  $\text{NaIO}_4$  was added to RM1 and the suspension was stirred at 40 °C for 48 h to afford the reaction mixture 2 (RM2) followed by filtration to obtain the filtrate and filter cake. The filtrate was evaporated to remove the solvent, dried in vacuum at 80 °C for 12 h, and then grinded into powder for use, which was denoted as the depolymerized mixtures (DMs).

**4.2.2. HPLC Analysis of the Depolymerized Products.** The real lignite depolymerized mixture (DM) was analyzed by HPLC (Shimadzu LC-20AT) as in our previous report.<sup>47,29</sup> A binary gradient elution procedure was used for the HPLC analysis. The mobile phase was acetonitrile and 0.1% (volume fraction) phosphoric acid aqueous solution, and the stationary phase was C18 bonded by silica gel (Shim-pack GIST C18, 5  $\mu\text{m}$ ). A UV detector at 235 nm was used to quantify the products. The mobile phase flow rate was 0.8 mL/min, and the column temperature was 45 °C. The gradient elution procedure was as follows: first, the volume ratio of acetonitrile to phosphoric acid aqueous was 5:95, the ratio was increased to 15:85 linearly over 10 min and then maintained for 38 min, and finally the ratio was decreased to 5:95 over 2 min. The HPLC profile of the DM was shown in Figure 12.

The detection results were shown in Figure 12. The depolymerization products mainly contain BHA (1,2,3,4,5,6-

benzenhexacarboxylic acid, peak no. 2), BPA (1,2,3,4,5-benzenepentacarboxylic acid, peak no. 3), 1,2,4,5-BTA (1,2,4,5-benzenetetracarboxylic acid, peak no. 4), 1,2,4-BTA (1,2,4-benzenetricarboxylic acid, peak no. 7), 1,2,3-BTA (1,2,4-benzenetricarboxylic acid, peak no. 8), and 1,2-BDA (1,2-benzenedicarboxylic acid, peak no. 9). Besides, peaks 5 and 6 may be isomers of 1,2,4,5-BTA.

**4.2.3. Preparation of the Zr-DM Catalyst in Water.** The Zr-based catalyst was prepared using depolymerized mixtures (DMs) and  $\text{ZrOCl}_2 \cdot 8\text{H}_2\text{O}$  as the raw materials. Typical procedures were as follows: a certain amount of DM and  $\text{ZrOCl}_2 \cdot 8\text{H}_2\text{O}$  was dissolved in 100 mL of distilled water, respectively. Then, the DM solution was dropwise slowly added into the solution of the Zr precursor, and the obtained mixture was further stirred at 80 °C for 5 h. Finally, the brown slurry was collected by centrifugation or filtration, washed for at least five times with distilled water and two times with ethanol until no  $\text{Cl}^-$  was detected by  $\text{AgNO}_3$ , dried in vacuum at 80 °C for 12 h, and then grinded into powder for use (denoted as Zr-DM).

The process for the preparation of the Zr-DM catalyst in DMF was similar to the above. One gram of DM was dissolved in 50 mL of DMF under room temperature, and then 1 g of  $\text{ZrCl}_4$  was added, forming solution A. Three grams of triethylamine was dissolved in 50 mL of DMF, forming solution B. Then, solution B was dropwise added into solution A under stirring. The mixture was maintained under room temperature for 3 h with stirring and then under 60 °C for 3 h without stirring. After this, the suspended slurry was separated by centrifugation to give a brown precipitate. Finally, the catalysts were obtained after the precipitate was thoroughly washed for two times with DMF and two times with ethanol, dried in vacuum at 80 °C for 12 h, and then grinded into powder for use.

**4.2.4. Preparation of the Cu-DM Catalyst.** The detailed preparing procedures of the Cu-DM catalyst were similar to our previous report.<sup>24</sup> In a typical procedure, a certain amount of DM and  $\text{Cu}(\text{OAc})_2 \cdot \text{H}_2\text{O}$  was separately dissolved in 50 mL of distilled water. Then, the two solutions were mixed and stirred at 30 °C for 3 h in the water bath kettle. After the reaction was finished, the precipitate of the mixture was separated by centrifugation and washed with distilled water for five times and ethanol for two times. The product was obtained after drying at 80 °C under vacuum for 12 h (denoted as Cu-DM).

**4.2.5. Preparation of Zr- and Cu-Organic Acid Catalysts.** To investigate the influences and contributions of the depolymerized products with different structures, single and pure carboxylic acids were used to construct Zr-carboxylic acid

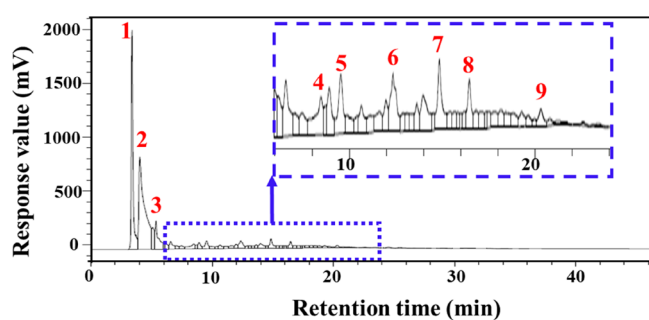


**Figure 12.** The HPLC profile of depolymerization products of lignite by RICO.

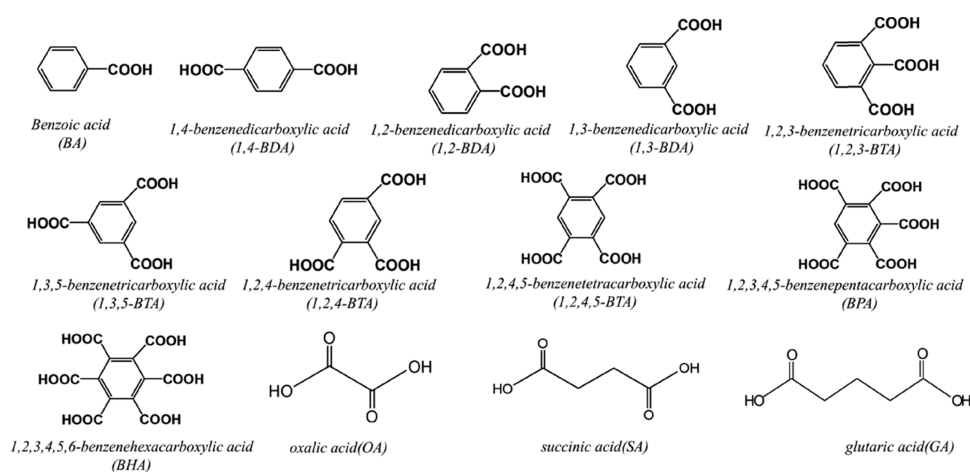


**Figure 13.** Structures and abbreviations of the typical organic acids in the depolymerized products of lignite by RICO.

catalysts. The preparation of Zr-based catalysts with carboxylic acids of different structures was similar to the preparation of Zr-DM. Due to the possibility that some depolymerized products with low contents may not be detected, 13 organic acids commonly obtained from oxidative depolymerization of lignite as shown in Figure 13 were selected to prepare the catalyst, respectively, to study the contribution and influence of different depolymerized components on the activity of the catalyst. Because some carboxylic acids were not easily soluble in water, the carboxylic acids were completely neutralized using sodium hydroxide solution before reacting with the zirconium precursor. In addition, as the number of carboxylic acid groups was known when the carboxylic acid monomer was used to construct the catalyst, the molar ratio of the zirconium precursor to carboxylic acid groups was controlled in accordance with the ratio of complete coordination (i.e., the molar ratio of  $Zr^{4+}$  to  $-COO^-$  was 1:4). The preparation of Cu-based catalysts with carboxylic acids of different structures was similar to that of the Cu-DM catalyst.

To facilitate subsequent research and discussion, the 13 kinds of zirconium-based catalysts prepared were denoted, respectively, as Zr-BA (Zr-benzoic acid), Zr-1,4-BDA (Zr-1,4-benzenedicarboxylic acid), Zr-1,2-BDA (Zr-1,2-benzenedicarboxylic acid), Zr-1,3-BDA (Zr-1,3-benzenedicarboxylic acid), Zr-1,2,4-BTA (Zr-1,2,4-benzenetricarboxylic acid), Zr-1,2,3-BTA (Zr-1,2,3-benzenetricarboxylic acid), Zr-1,3,5-BTA (Zr-1,3,5-benzenetricarboxylic acid), Zr-1,2,4,5-BTA (Zr-1,2,4,5-benzenetetracarboxylic acid), Zr-BPA (Zr-1,2,3,4,5-benzenepentacarboxylic acid), Zr-BHA (Zr-1,2,3,4,5,6-benzenehexacarboxylic acid), Zr-OA (Zr-oxalic acid), Zr-SA (Zr-succinic acid), and Zr-GA (Zr-glutaric acid).

Cu-based catalysts prepared by each carboxylic acid were denoted as Cu-BA (Cu-benzoic acid), Cu-1,4-BDA (Cu-1,4-benzenedicarboxylic acid), Cu-1,2-BDA (Cu-1,2-benzenedicarboxylic acid), Cu-1,3-BDA (Cu-1,3-benzenedicarboxylic acid), Cu-1,2,4-BTA (Cu-1,2,4-benzenetricarboxylic acid), Cu-1,3,5-BTA (Cu-1,3,5-benzenetricarboxylic acid), Cu-1,2,4,5-BTA (Cu-1,2,4,5-benzenetetracarboxylic acid), Cu-BPA (Cu-1,2,3,4,5-benzenepentacarboxylic acid), Cu-BHA (Cu-1,2,3,4,5,6-benzenehexacarboxylic acid), Cu-OA (Cu-oxalic acid), and Cu-SA (Cu-succinic acid) catalyst.

**4.3. Catalyst Characterization.** Scanning electron microscopy (SEM) measurements were performed on a Hitachi SU8220 scanning electron microscope operated at 20 kV with

an energy dispersive spectrometer (EDS) apparatus. X-ray diffraction (XRD) was carried out via an XD8 Advance-Bruker AXS X-ray diffractometer using  $Cu K\alpha$  radiation ( $\lambda = 532$  nm) and Ni filter scanning at  $2^\circ/\text{min}$  ranging from  $5$  to  $90^\circ$ . The tube voltage was 40 kV, and the current was 40 mA. Fourier transform infrared (FT-IR) spectra were obtained using a PerkinElmer spectrometer. The XPS measurements were carried out via an ESCALAB 250Xi spectrometer (Thermo Fisher Scientific) at a pressure of  $3 \times 10^{-9}$  mbar using  $Al K\alpha$  as the excitation source ( $h\nu = 1486.6$  eV) and operating at 15 kV and 150 W. The thermogravimetric (TG) analysis of the catalyst was performed using a thermogravimetric analysis system (Diamond TG/DTA6300, PerkinElmer Instruments) under an  $N_2$  atmosphere at a heating rate of  $10^\circ C \text{ min}^{-1}$ . The specific surface area was calculated by the BET method, and mesopore volume was derived from the adsorption isotherm according to the Barrett–Joyner–Halenda (BJH) model. All calculations were based on the adsorption isotherms. Inductively coupled plasma-optical emission spectrometry (ICP-OES) was carried out via the Thermo Fisher Scientific iCAP 7000.

**4.4. Reaction.** **4.4.1. The Reaction of the Catalytic Transfer Hydrogenation of Furfural over Zr-DM.** Typically, furfural (1 mmol), isopropanol (5 mL), and the quantitative catalyst were introduced into a 15 mL Teflon-lined stainless steel autoclave equipped with a magnetic stirrer. After sealing, the reaction mixture was stirred and allowed to react at the suitable temperature for the desired time. After reaction, the reactor was cooled down in cold water to quench the reaction, and the reaction solution was transferred and diluted by isopropanol. The samples were analyzed quantitatively by gas chromatography (Techcomp GC7900) with a flame ionization detector using decane as the internal standard. Identification of the products and the reactant was done using a GC–MS (Shimadzu QP 2010) as well as by comparing the retention times with respective standards in GC traces.

**4.4.2. The Reaction of Selective Oxidation of Various Alcohols into Aldehydes over Cu-DM.** Taking the conversion of benzyl alcohol to benzaldehyde for example, a 15 mL Teflon-lined stainless steel autoclave equipped with a magnetic stirrer was used to perform the reaction. In a typical experiment, benzyl alcohol (1 mmol), TEMPO (0.5 mmol),  $Na_2CO_3$  (1 mmol), DMF (5 mL), and 160 mg of the catalyst were loaded into the reactor. After the reactor was sealed, it

was placed in an oil bath pot to react at the desired temperature and time. When the reaction finished, the reactor was cooled down in ice water to quench the reaction, and the reaction solution was transferred and diluted by DMF. The analysis and identification of the products and the reactant were done using the same methods as the Zr-DM catalyst.

**4.5. Catalyst Heterogeneity and Recycles.** To check the heterogeneity of the catalysts, the solid catalysts were removed from the reaction mixture after reaction for a short time, and the supernatant was allowed to react to see if the product yield could further increase with the absence of the solid catalysts. In the reusability experiments, the catalyst was separated by centrifugation, washed with fresh isopropanol for three times, and then reused for the next run without further treatments.

## ■ ASSOCIATED CONTENT

### SI Supporting Information

The Supporting Information is available free of charge at <https://pubs.acs.org/doi/10.1021/acsomega.1c00766>.

Studies of the preparation conditions of the Cu-DM catalyst (S1), characterization results of the Cu-DM catalyst (S2), activity comparison of Cu-DM with other benzyl alcohol oxidation catalysts (S3), and heterogeneity and reusability of Cu-DM catalysts (S4) (PDF)

## ■ AUTHOR INFORMATION

### Corresponding Authors

**Jianxiu Hao** – Chemical Engineering, Inner Mongolia University of Technology; Inner Mongolia Key Laboratory of High-Value Functional Utilization of Low Rank Carbon Resources, Hohhot 010051, China; [orcid.org/0000-0001-9841-329X](https://orcid.org/0000-0001-9841-329X); Email: [hjx2020@imut.edu.cn](mailto:hjx2020@imut.edu.cn)

**Quansheng Liu** – Chemical Engineering, Inner Mongolia University of Technology; Inner Mongolia Key Laboratory of High-Value Functional Utilization of Low Rank Carbon Resources, Hohhot 010051, China; [orcid.org/0000-0001-7763-7569](https://orcid.org/0000-0001-7763-7569); Email: [liuqs@imut.edu.cn](mailto:liuqs@imut.edu.cn)

### Authors

**Limin Han** – Chemical Engineering, Inner Mongolia University of Technology; Inner Mongolia Key Laboratory of High-Value Functional Utilization of Low Rank Carbon Resources, Hohhot 010051, China; Present

Address: Present address: Wuhai Vocational & Technical College, Wuhai 010070, Inner Mongolia, China (L.H.).

**Keli Yang** – Chemical Engineering, Inner Mongolia University of Technology; Inner Mongolia Key Laboratory of High-Value Functional Utilization of Low Rank Carbon Resources, Hohhot 010051, China

**Na Li** – Chemical Engineering, Inner Mongolia University of Technology; Inner Mongolia Key Laboratory of High-Value Functional Utilization of Low Rank Carbon Resources, Hohhot 010051, China

**Runxia He** – Chemical Engineering, Inner Mongolia University of Technology; Inner Mongolia Key Laboratory of High-Value Functional Utilization of Low Rank Carbon Resources, Hohhot 010051, China

**Keduan Zhi** – Chemical Engineering, Inner Mongolia University of Technology; Inner Mongolia Key Laboratory of High-Value Functional Utilization of Low Rank Carbon

Resources, Hohhot 010051, China; [orcid.org/0000-0002-8307-6822](https://orcid.org/0000-0002-8307-6822)

Complete contact information is available at: <https://pubs.acs.org/10.1021/acsomega.1c00766>

### Notes

The authors declare no competing financial interest.

## ■ ACKNOWLEDGMENTS

This work was supported by the National Natural Science Foundation of China (21676149, 21868021, and 21868020), the Science and Research Projects of Inner Mongolia University of Technology (IMUT) (ZY202004), the Natural Science Foundation of Inner Mongolia (2019MS02025), and the Startup Fund for New Teachers of IMUT.

## ■ REFERENCES

- (1) Song, C. S. Fuel processing for low-temperature and high-temperature fuel cells: Challenges, and opportunities for sustainable development in the 21st century. *Catal. Today* **2002**, *77*, 17–49.
- (2) He, M. Y.; Sun, Y. H.; Han, B. X. Green carbon science: scientific basis for integrating carbon resource processing, utilization, and recycling. *Angew. Chem., Int. Ed.* **2013**, *52*, 9620–9633.
- (3) Li, Z. K.; Wei, X. Y.; Yan, H. L.; Wang, Y. G.; Kong, J.; Zong, Z. M. Advances in lignite extraction and conversion under mild conditions. *Energy Fuel* **2015**, *29*, 6869–6886.
- (4) Zhou, Q.; Zou, T.; Zhong, M.; Zhang, Y. M.; Wu, R. C.; Gao, S. Q.; Xu, G. W. Lignite upgrading by multi-stage fluidized bed pyrolysis. *Fuel Process. Technol.* **2013**, *116*, 35–43.
- (5) Yu, J. L.; Tahmasebi, A.; Han, Y. N.; Yin, F. K.; Li, X. C. A review on water in low rank coals: The existence, interaction with coal structure and effects on coal utilization. *Fuel Process. Technol.* **2013**, *106*, 9–20.
- (6) Liu, F. J.; Wei, X. Y.; Gui, J.; Li, P.; Wang, Y. G.; Li, W. T.; Zong, Z. M.; Xing, F.; Zhao, Y. P. Characterization of organonitrogen species in Xianfeng lignite by sequential extraction and ruthenium ion-catalyzed oxidation. *Fuel Process. Technol.* **2014**, *126*, 199–206.
- (7) Lv, J. H.; Wei, X. Y.; Qing, Y.; Wang, Y. H.; Wen, Z.; Zhu, Y.; Wang, Y. G.; Zong, Z. M. Insight into the structural features of macromolecular aromatic species in Huoliuguole lignite through ruthenium ion-catalyzed oxidation. *Fuel* **2014**, *128*, 231–239.
- (8) Liu, F. J.; Wei, X. Y.; Fan, M. H.; Zong, Z. M. Separation and structural characterization of the value-added chemicals from mild degradation of lignites: A review. *Appl Energy* **2016**, *170*, 415–436.
- (9) Wang, W. H.; Hou, Y. C.; Wu, W. Z.; Niu, M. G.; Liu, W. N. Production of Benzene Polycarboxylic Acids from Lignite by Alkali-Oxygen Oxidation. *Ind. Eng. Chem. Res.* **2012**, *51*, 14994–15003.
- (10) Wang, W. H.; Hou, Y. C.; Wu, W. Z.; Niu, M. G. Simultaneous production of small-molecule fatty acids and benzene polycarboxylic acids from lignite by alkali-oxygen oxidation. *Fuel Process. Technol.* **2013**, *112*, 7–11.
- (11) Wang, Y. G.; Wei, X. Y.; Yan, H. L.; Liu, F. J.; Li, P.; Zong, Z. M. Sequential oxidation of Jincheng No. 15 anthracite with aqueous sodium hypochlorite. *Fuel Process. Technol.* **2014**, *125*, 182–189.
- (12) Wood, B. J.; Sancier, K. M. The mechanism of the catalytic gasification of coal char: A critical review. *Catal Rev* **1984**, *26*, 233–279.
- (13) Huang, Y. G.; Zong, Z. M.; Yao, Z. S.; Zheng, Y. X.; Mou, J.; Liu, G. F.; Gao, J. P.; Ding, M. J.; Cai, K. Y.; Wang, F.; Wei, Z.; Xia, Z. L.; Wu, L.; Wei, X. Y. Ruthenium ion-catalyzed oxidation of Shenfu coal and its residues. *Energy Fuel* **2008**, *22*, 1799–1806.
- (14) Liu, F. J.; Wei, X. Y.; Zhu, Y.; Gui, J.; Wang, Y. G.; Fan, X.; Zhao, Y. P.; Zong, Z. M.; Zhao, W. Investigation on structural features of Shengli lignite through oxidation under mild conditions. *Fuel* **2013**, *109*, 316–324.

- (15) Wang, Y. G.; Wei, X. Y.; Xie, R. L.; Liu, F. J.; Li, P.; Zong, Z. M. Structural Characterization of Typical Organic Species in Jincheng No. 15 Anthracite. *Energ Fuel* **2015**, *29*, 595–601.
- (16) Miura, K. Mild conversion of coal for producing valuable chemicals. *Fuel Process. Technol.* **2000**, *62*, 119–135.
- (17) Hayashi, J.; Matsuo, Y.; Kusakabe, K.; Morooka, S. Depolymerization of lower rank coals by low-temperature O<sub>2</sub> oxidation. *Energ Fuel* **1997**, *11*, 227–235.
- (18) Arul Leo Bastin, J.; Krishnamurthy, N.; Madhavan, D.; Vallinayagam, P.; Palanichamy, M.; Chellamani, A. Chromatographic separation of alkylated depolymerized Neyveli lignite. *Solid Fuel Chem.* **2017**, *51*, 256–266.
- (19) Hou, Y. C.; Li, J.; Ren, S. H.; Niu, M. G.; Wu, W. Z. Separation of the isomers of benzene poly(carboxylic acid)s by quaternary ammonium salt via formation of deep eutectic solvents. *J. Phys. Chem. B* **2014**, *118*, 13646–13650.
- (20) Kawamura, K.; Takahashi, K.; Okuwaki, A. Influence of pH and diluent on the Ion-pair solvent extraction of aromatic carboxylic acids using quaternary ammonium salts. *Sep. Sci. Technol.* **2006**, *41*, 2795–2806.
- (21) Kawamura, K.; Okuwaki, A.; Verheyen, T. V.; Perry, G. J. Separation of aromatic carboxylic acids using quaternary ammonium salts on reversed-phase HPLC. 2. Application for the analysis of Loy Yang coal oxidation products. *Sep. Sci. Technol.* **2006**, *41*, 723–732.
- (22) Zhou, C. L.; Liu, Q. S.; Li, Y.; Teng, Y. Y.; Zhi, K. D.; Song, Y. M.; He, R. X. Influence of pyrolysis temperature on the gaseous products of lignite. *Adv. Mater. Res.* **2012**, *524-527*, 883–886.
- (23) Hao, J. X.; Han, L. M.; Sha, Y. F.; Yu, X. X.; Liu, H. Y.; Ma, X. Y.; Yang, Y. Z.; Zhou, H. C.; Liu, Q. S. Facile use of lignite as robust organic ligands to construct Zr-based catalysts for the conversion of biomass derived carbonyl platforms into alcohols. *Fuel* **2019**, *239*, 1304–1314.
- (24) Sha, Y. F.; Li, N.; Zhi, K. D.; Song, Y. M.; Liu, Q. S.; Zhou, H. C. Novel and Efficient Cu-based Catalyst Constructed by Lignite Alkali-Oxygen Oxidation Products for Selective Aerobic Oxidation of Alcohols to Aldehydes. *Fuel* **2019**, *257*, 116042.
- (25) Xiao, Z. H.; Zhou, H. C.; Hao, J. M.; Hong, H. L.; Song, Y. M.; He, R. X.; Zhi, K. D.; Liu, Q. S. A novel and highly efficient Zr-containing catalyst based on humic acids for the conversion of biomass-derived ethyl levulinate into gamma-valerolactone. *Fuel* **2017**, *193*, 322–330.
- (26) Zhang, B. B.; Hao, J. X.; Sha, Y. F.; Zhou, H. C.; Yang, K. L.; Song, Y. M.; Ban, Y. P.; He, R. X.; Liu, Q. S. Utilization of lignite derivatives to construct Zr-based catalysts for the conversion of biomass-derived ethyl levulinate. *Fuel* **2018**, *217*, 122–130.
- (27) Iglesias, J.; Melero, J.; Morales, G.; Moreno, J.; Segura, Y.; Paniagua, M.; Cambra, A.; Hernandez, B. Zr-SBA-15 Lewis acid catalyst: activity in Meerwein Ponndorf Verley reduction. *Catalysts* **2015**, *5*, 1911–1927.
- (28) Zhou, H. C.; Sha, Y. F.; Xiao, Z. H.; Li, L.; Hao, J. M.; Yang, K. L.; Li, N.; He, R. X.; Liu, Q. S. Using benzene carboxylic acids to prepare zirconium-based catalysts for the conversion of biomass-derived furfural. *Int. J. Coal Sci. Technol.* **2018**, *1*, 1–9.
- (29) Sha, Y. F.; Xiao, Z. H.; Zhou, H. C.; Yang, K. L.; Song, Y. M.; Li, N.; He, R. X.; Zhi, K. D.; Liu, Q. S. Direct use of humic acid mixtures to construct efficient Zr-containing catalysts for Meerwein–Ponndorf–Verley reactions. *Green Chem.* **2017**, *19*, 4829–4837.
- (30) Song, J. L.; Zhou, B. W.; Zhou, H. C.; Wu, L. Q.; Meng, Q. L.; Liu, Z. M.; Han, B. X. Porous zirconium-phytic acid hybrid: a highly efficient catalyst for Meerwein–Ponndorf–Verley reductions. *Angew. Chem., Int. Ed.* **2015**, *54*, 9399–9403.
- (31) Li, H.; He, J.; Riisager, A.; Saravanamurugan, S.; Song, B.; Yang, S. Acid–base bifunctional zirconium N-alkyltriphosphate nanohybrid for hydrogen transfer of biomass-derived carboxides. *ACS Catal.* **2016**, *6*, 7722–7727.
- (32) Wang, F.; Zhang, Z. H. Catalytic Transfer Hydrogenation of Furfural into Furfuryl Alcohol over Magnetic  $\gamma$ -Fe<sub>2</sub>O<sub>3</sub>@HAP Catalyst. *ACS Sustainable Chem. Eng.* **2017**, *5*, 942–947.
- (33) Li, J.; Liu, J. L.; Zhou, H. J.; Fu, Y. Catalytic transfer hydrogenation of furfural to furfuryl alcohol over nitrogen-doped carbon-supported iron catalysts. *ChemSusChem* **2016**, *9*, 1339–1347.
- (34) Reddy Kannapu, H. P.; Mullen, C. A.; Elkasabi, Y.; Boateng, A. A. Catalytic transfer hydrogenation for stabilization of bio-oil oxygenates: Reduction of p-cresol and furfural over bimetallic Ni–Cu catalysts using isopropanol. *Fuel Process. Technol.* **2015**, *137*, 220–228.
- (35) Biradar, N. S.; Hengne, A. M.; Sakate, S. S.; Swami, R. K.; Rode, C. V. Single pot transfer hydrogenation and aldolization of furfural over metal oxide catalysts. *Catal. Lett.* **2016**, *146*, 1611–1619.
- (36) Yuan, Q. Q.; Zhang, D. M.; Haandel, L. V.; Ye, F. Y.; Xue, T.; Hensen, E. J. M.; Guan, Y. Y. Selective liquid phase hydrogenation of furfural to furfuryl alcohol by Ru/Zr-MOFs. *J. Mol. Catal. A-Chem* **2015**, *406*, 58–64.
- (37) Bhogeswararao, S.; Srinivas, D. Catalytic conversion of furfural to industrial chemicals over supported Pt and Pd catalysts. *J. Catal.* **2015**, *327*, 65–77.
- (38) Chen, X. F.; Zhang, L. G.; Zhang, B.; Guo, X. C.; Mu, X. D. Highly selective hydrogenation of furfural to furfuryl alcohol over Pt nanoparticles supported on g-C<sub>3</sub>N<sub>4</sub> nanosheets catalysts in water. *Sci Rep-UK* **2016**, *6*, 276–282.
- (39) Halilu, A.; Ali, T. H.; Atta, A. Y.; Sudarsanam, P.; Bhargava, S. K.; Abd Hamid, S. B. Highly selective hydrogenation of biomass-derived furfural into furfuryl alcohol using a novel magnetic nanoparticles catalyst. *Energ Fuel* **2016**, *30*, 2216–2226.
- (40) Audemar, M.; Ciotonea, C.; Vigier, K. D. O.; Royer, S.; Ungureanu, A.; Dragoi, B.; Dumitriu, E.; Jerome, F. Selective hydrogenation of furfural to furfuryl alcohol in the presence of a recyclable cobalt/SBA-15 catalyst. *ChemSusChem* **2015**, *8*, 1885–1891.
- (41) Kotbagi, T. V.; Gurav, H. R.; Nagpure, A. S.; Chilukuri, S. V.; Bakker, M. G. Highly efficient nitrogen-doped hierarchically porous carbon supported Ni nanoparticles for the selective hydrogenation of furfural to furfuryl alcohol. *RSC Adv.* **2016**, *6*, 67662–67668.
- (42) Wu, J.; Gao, G.; Li, J. L.; Sun, P.; Long, X. D.; Li, F. W. Efficient and versatile CuNi alloy nanocatalysts for the highly selective hydrogenation of furfural. *Appl Catal B- Environl* **2017**, *203*, 227–236.
- (43) Yan, K.; Wu, X.; An, X.; Xie, X. M. Novel preparation of nano-composite CuO-Cr<sub>2</sub>O<sub>3</sub> using CTAB-template method and efficient for hydrogenation of biomass-derived furfural. *Funct Mater Lett* **2013**, *06*, 1–5.
- (44) Song, J. L.; Wu, L. Q.; Zhou, B. W.; Zhou, H. C.; Fan, H. L.; Yang, Y. Y.; Meng, Q. L.; Han, B. X. A new porous Zr-containing catalyst with a phenate group: an efficient catalyst for the catalytic transfer hydrogenation of ethyl levulinate to  $\gamma$ -valerolactone. *Green Chem.* **2015**, *17*, 1626–1632.
- (45) Zhou, H. C.; Song, J. L.; Meng, Q. L.; He, Z. H.; Jiang, Z. W.; Zhou, B. W.; Liu, H. Z.; Han, B. X. Cooperative catalysis of Pt/C and acid resin for the production of 2,5-dimethyltetrahydrofuran from biomass derived 2,5-hexanedione under mild conditions. *Green Chem.* **2015**, *18*, 220–225.
- (46) Li, N.; Li, Y.; Zhou, H. C.; Liu, Y.; Song, Y. M.; Zhi, K. D.; He, R. X.; Yang, K. L.; Liu, Q. S. Direct production of high hydrogen syngas by steam gasification of Shengli lignite/chars: Significant catalytic effect of calcium and its possible active intermediate complexes. *Fuel* **2017**, *203*, 817–824.
- (47) Hao, J. X.; Han, L. M.; Yang, K. L.; Zhao, H. Y.; Li, X. M.; Ban, Y. P.; Li, N.; Zhou, H. C.; Liu, Q. S. Metal ion-induced separation of valuable organic acids from a depolymerized mixture of lignite without using organic solvents. *RSC Adv.* **2020**, *10*, 3479–3486.